

# Supplemental Information

## Probing the Dissociation of Protein Complexes by means of Gas-Phase H/D Exchange Mass Spectrometry

Ulrik H. Mistarz,<sup>1,⊥</sup> Shane A. Chandler,<sup>2,⊥</sup> Jeffery M. Brown,<sup>3</sup> Justin L.P. Benesch<sup>2,\*</sup> and Kasper D. Rand<sup>1,\*</sup>

<sup>1</sup>Department of Pharmacy, University of Copenhagen, Universitetsparken 2, Denmark.

<sup>2</sup>Physical & Theoretical Chemistry Laboratory, Department of Chemistry, University of Oxford, U.K.

<sup>3</sup>Waters Corporation, Stamford Avenue, Altrincham Road, U.K.

<sup>⊥</sup>Contributed equally

*Correspondence to:*

Justin L.P. Benesch; *e-mail:* [justin.benesch@chem.ox.ac.uk](mailto:justin.benesch@chem.ox.ac.uk)

Kasper D. Rand; *e-mail:* [kasper.rand@sund.ku.dk](mailto:kasper.rand@sund.ku.dk)

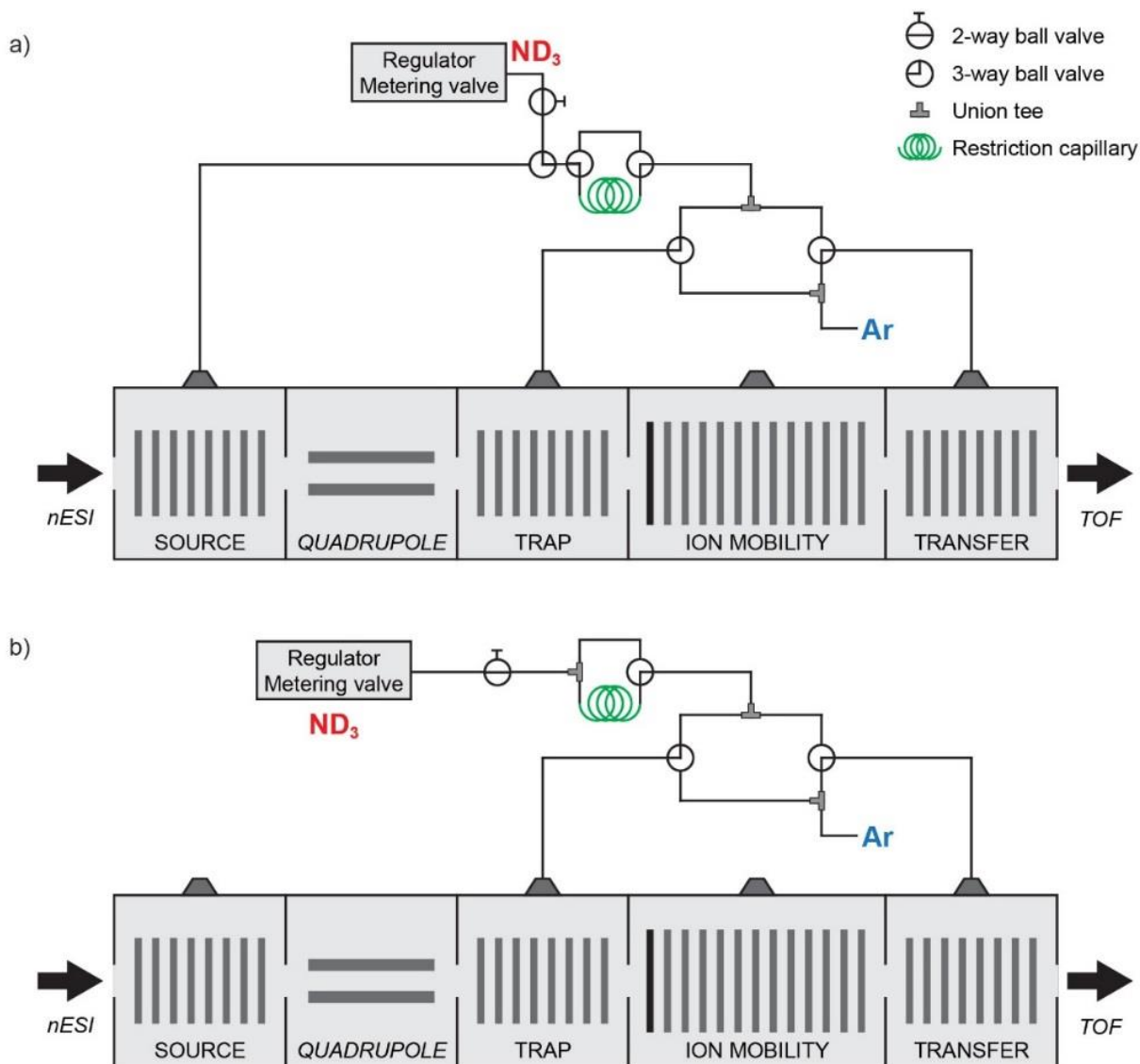


**Figure S-1.** Modifications to the Synapt G1 and Synapt G2 hybrid Q-TOF mass spectrometers, to allow the introduction of deuterated ammonia gas ( $\text{ND}_3$ -gas) into various T-wave ions guides (TWIG) of the instruments. Modifications and installation of stainless steel tubing installed on Synapt G2 (a) and Synapt G1 (b) Q-TOF instruments are shown. The setup installed on the Synapt G2 enables gas-phase HDX-MS in either source, trap or transfer T-Wave ion guide (TWIG). Where the setup on the Synapt G1 enables gas-phase HDX-MS to be performed in either the trap or transfer TWIG. This can be changed or switched on/off by simply turning switching valves located outside the instrument. To ease the control of  $\text{ND}_3$ -gas, especially at lower gas pressure, restriction capillary consisting of three PEEKSil 50cm x 1/16", 100  $\mu\text{M}$  (Sigma) in tandem by 1/16"-1/16" connectors (SS-100-6) which was connected between the regulator and mass spectrometer.

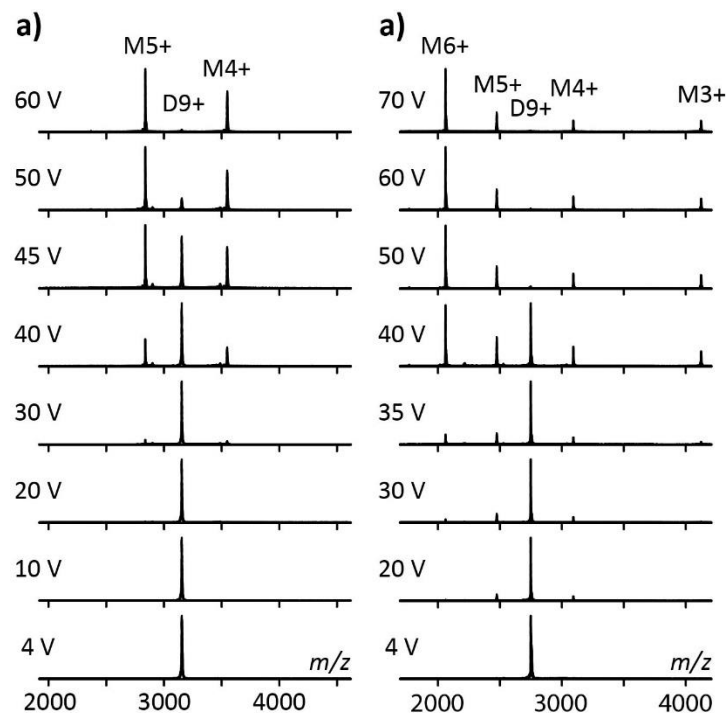


**Figure S-2.** Gas-phase dissociation of protein dimers at increasing collision energies. Experiments were performed with  $\text{ND}_3$ -labeling in the trap TWIG with subsequent gas-phase dissociation in the transfer TWIG. Mass spectra is shown for A)  $\alpha$ -lactalbumin 9+ dimer (4–60 V CID) and B) cytochrome *c* 9+ dimer (4–70 V CID). The 9+ dimer (D9+) and dissociated monomers at charge states 3–6+ (M3+, M4+, M5+, M6+) are annotated in the figure

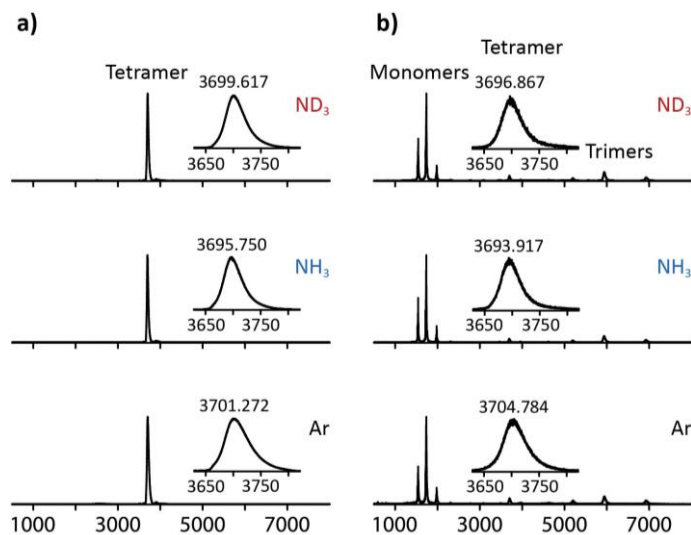


**Figure S-3.** Effect of different gasses on the peak shape of transthyretin (TTR). Quadrupole selected 15+ tetramer of TTR with (a) and without (b) gas-phase complex dissociation in the transfer TWIG, by transfer CE of 4 V and 40 V, respectively. Similar experiments were performed with either  $\text{ND}_3$ -gas (top),  $\text{NH}_3$ -gas (middle), or Ar-gas (bottom) in the trap TWIG

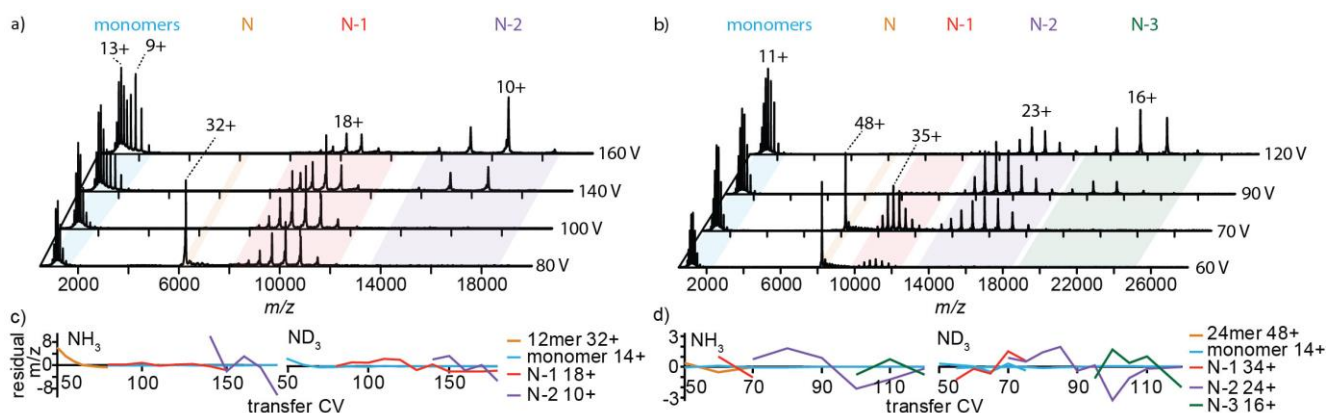


**Figure S-4.** Gas-phase dissociation of HSP16.9 and HSP16.5 at increasing collision energies. The intact isolated complex was labelled with ND<sub>3</sub>-gas in the trap TWIG with subsequent gas-phase dissociation in the transfer TWIG. Mass spectra are shown for a) HSP16.9 32+ 12mer (80–160 V CID) and b) HSP16.5 48+ 24mer (60–120 V CID). Sequential subunit loss occurs in both cases resulting in N-1, N-2 and, in the case of HSP16.5, N-3 stripped oligomers in addition to the corresponding monomers. No systematic variation in  $m/z$  centroid was observed at increasing collision energy for either HSP16.9 or HSP16.5 under exposure to either NH<sub>3</sub>-gas or ND<sub>3</sub>-gas. The deviation in peak centroid, relative to the value averaged across all collision voltages, is shown in both gases for c) HSP16.9 and d) HSP16.5. Monomers, show highly consistent behavior across all collision voltages. (Oligomeric regions have been scaled by 5, >8000  $m/z$ , for HSP16.9 and scaled by 8 for collision voltages 70–120 V, >6000  $m/z$ , for HSP 16.5)

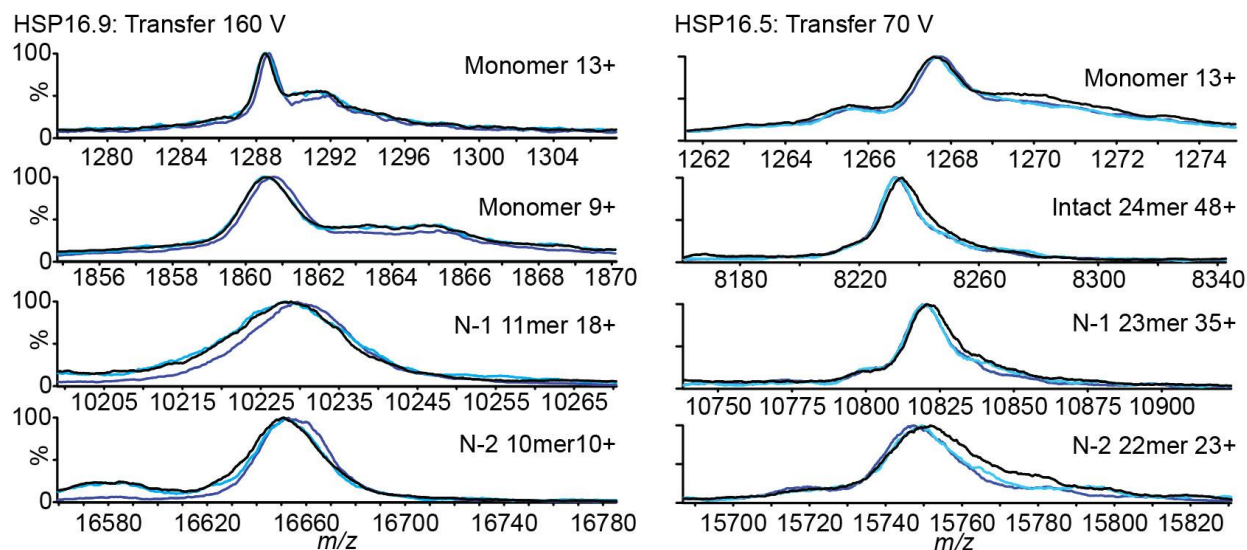


**Figure S-5.** Example mass spectra for HSP16.9 (left) and HSP16.5 (right) showing the reproducibility of gas-phase labelled oligomers after CID. Three replicates for selected species and charges states are shown corresponding to the data in Fig. 4

	HSP16.9		HSP16.5	
	number of labile Hs		number of labile Hs	
Residue	Seq.	SA	Seq.	SA
C	0	0	0	0
D	10	4	5	3
E	18	11	17	11
H	2	0	1	1
K	30	22	22	14
R	44	4	24	8
S	11	1	12	7
T	5	3	9	2
Y	0	0	2	0
termini	3	1	3	1
Subunit total	123	46	95	47
Complex total	1476	552	2280	1128
Complex total + z	1508	584	2328	1176

**Table S-1.** Determination of the number of labile hydrogens expected for HSP16.9 and HSP16.5 based on the sequence (Seq.) and surface accessible (SA) residues from the crystal structures, 1GME and 1SHS respectively. The contribution from different residues are summarised for each model and the total determined for the intact complex including charge (z)

Model	HSP16.9		HSP16.5	
	Labile Hs	F <sub>D</sub>	Labile Hs	F <sub>D</sub>
Seq.+BB	3320	0.04	5880	0.05
Seq.	1508	0.09	2328	0.12
SA	584	0.24	1176	0.24
SA+SB	548	0.25	936	0.30

**Table S-2.** Approximation of the deuteron fraction (F<sub>D</sub>) of HSP16.9 and HSP16.5. The F<sub>D</sub> is based on the total number of labile hydrogens for different models discussed in the main text; sequence and the backbone (Seq.+BB), sequence (Seq.), surface accessible (SA) and surface accessible including salt-bridges (SA+SB)